Journal of Cell Science 104, 929-938 (1993)
Printed in Great Britain © The Company of Biologists Limited 1993

Degradation of an extracellular matrix: sea urchin hatching enzyme removes cortical granule-derived proteins from the fertilization envelope

Nancy M. Mozingo*, Lisa R. Hollar and Douglas E. Chandler

Department of Zoology, Arizona State University, Tempe, Arizona 85287-1501, USA

*Author for correspondence

SUMMARY

The sea urchin fertilization envelope is an extracellular matrix assembled at fertilization to prevent polyspermy and protect the embryo during early development. During hatching, the embryo secretes a proteolytic hatching enzyme which dissolves the fertilization envelope, allowing a ciliated blastula to swim free. In this study we examined ultrastructural changes in the fertilization envelope during degradation of this matrix by hatching enzyme. The completed fertilization envelope is a trilaminar structure consisting of a dense, central layer of filaments sandwiched between surface coats of paracrystalline material. Hatching enzyme disassembles this matrix by degrading the paracrystalline layers and removing macromolecules from the central layer leaving behind a thin matrix of loosely woven fibers.

Key words: hatching, sea urchin eggs, fertilization envelope, *Lytechinus pictus*, *Strongylocentrotus purpuratus*, freeze-fracture

INTRODUCTION

The sea urchin fertilization envelope (FE) is a complex, extracellular matrix assembled at fertilization to guard against polyspermy and to protect the fragile embryo until it hatches out of the FE as a ciliated blastula (Ishida, 1936). The FE is assembled when cortical granule secretions modify and assimilate into the vitelline layer, a glycoproteinaceous layer surrounding unfertilized eggs (Glabe and Vacquier, 1978; Kinsey and Lennarz, 1981; Rossignol et al., 1984). The completed FE is remarkably resistant to solubilization by various chemical, mechanical and enzymatic treatments (reviewed by Kay and Shapiro, 1985); indeed the proteolytic hatching enzyme secreted by blastula stage embryos appears to be the only enzyme which can effectively degrade this structure (Ishida, 1936; Barrett and Edwards, 1976).

The first step in FE assembly occurs when covalent attachments between the vitelline layer and the egg plasma membrane are severed, allowing the vitelline layer to elevate from the egg surface (Vacquier et al., 1972; Longo and Schuel, 1973; Carroll and Epel, 1975). In some sea urchin species the elevated vitelline layer retains casts of the microvilli it once covered (Veron et al., 1977; Chandler and Heuser, 1980; Carroll and Cohen, 1990), while in other species the vitelline layer appears to flatten out during elevation (Schuel et al., 1982; Carroll and Cohen, 1990; Mozingo and Chandler, 1992). Initially, the elevated vitelline layer is a thin matrix consisting of loosely woven fibers; however, the appearance of this structure is dramatically altered between 2 and 5 minutes after fertilization. First, the vitelline scaffold is filled in and thickened with cortical granule secretions (Chandler and Heuser, 1980; Mozingo and Chandler, 1992). Next, paracrystalline coating arises when ordered rows of macromolecules are deposited on either side of the thickened structure (Chandler and Heuser, 1980; Chandler and Kazilek, 1986). Thus, the assembled FE is trilaminar, consisting of a dense central layer sandwiched between surface coats of paracrystalline material.

Many of the ultrastructural corollaries of specific enzymes involved in FE assembly have been identified. For instance, proteases released from cortical granules allow vitelline layer elevation by severing vitelline posts (Longo and Schuel, 1973; Carroll and Epel, 1975; Mozingo and Chandler, 1991), the structures which connect the egg plasma membrane with the vitelline layer (Kidd, 1978; Chandler and Heuser, 1980). In addition, the enzyme ovoperoxidase appears to be required for paracrystalline protein coating. This enzyme, secreted by cortical granules at fertilization, is responsible for “hardening” the FE by incorporating dityrosine cross-links into the nascent FE (Foerder and Shapiro, 1977; Hall, 1978). When ovoperoxidase is inhibited, the vitelline scaffold never obtains a normal paracrystalline coat, suggesting the ultrastructural consequence of ovoperoxidase activity is cross-linking of paracrystalline material into the vitelline scaffold (Mozingo and Chandler, 1991).

Although hatching enzymes have been isolated from several different sea urchin species (Barrett and Edwards, 1976; Takeuchi et al., 1979; Lepage and Gache, 1989), the effects of hatching enzyme on FE structure have not pre-

viously been described. In this study, we examined the changes in FE ultrastructure which occur due to proteolytic degradation by hatching enzyme, both in vivo and in vitro. We found that hatching enzyme attacks the paracrystalline layers and removes macromolecules from the central layer, leaving behind a thin fibrous structure reminiscent of an elevated vitelline layer which has not been modified by cortical granule secretions. Certain aspects of the FE disassembly process are reminiscent of FE assembly, since it appears that a subset of the cortical granule proteins cross-linked into the vitelline scaffold by ovoperoxidase at fertilization are targeted for removal by hatching enzyme.

MATERIALS AND METHODS

Gametes and embryo culture

Strongylocentrotus purpuratus or *Lytechinus pictus* were purchased from Marinus (Long Beach, CA) and maintained in Tropic Marin seawater (TMSW; Dr Biener GMBH, Wartenburg, West Germany). Gametes were shed by introducing 0.5-2 ml of 0.5 M KCl into the body cavity. Eggs were collected in Tropic Marin seawater and poured through a 100 μm mesh nylon cloth to remove spines and other debris. Sperm was collected "dry" in plastic Petri dishes and kept on ice until immediately before use. Sperm (0.002%) was added to a suspension of eggs (10%, v/v) in TMSW and gently stirred for 30 seconds after addition. After 10 minutes, the embryo suspension was diluted with TMSW to 1% and maintained at 16°C until hatching. In some cases Streptomycin and Penicillin G were added at 50 μg/ml each.

Hatching enzyme was collected as described by Barrett and Edwards (1976). Just prior to hatching, the embryo culture was concentrated approximately 10-fold, and after hatching was complete the culture media was collected. After filtration through Whatman # 1 chromatography paper, the filtrate was concentrated approximately 10-fold by Amicon ultrafiltration using a PM-10 membrane. The ability of this ultrafiltrate to dissolve FEs was monitored with light microscopy; the FE of 2-cell stage embryos disappeared within 2 hours when incubated with the ultrafiltrate (data not shown).

Scanning electron microscopy

Prior to hatching, aliquots of embryos were pipetted onto polylysine-coated mica squares or Nickel hole grids (for viewing in a Philips CM12S microscope) and allowed to adhere for 15 minutes. Mica squares or grids with adherent embryos were then placed in TMSW and allowed to hatch. Hatching embryos were fixed for 1.5 hours on ice in a glutaraldehyde/osmium tetroxide/ruthenium red cocktail, as described by Morrill (1986). Samples were washed in ice-cold ASW (1×) and distilled H_2O (2×) and then dehydrated in a graded ethanol series. Samples were dried using Peldri II (Ted Pella, Inc., Redding, CA), sputter-coated with gold and viewed with an AMR 1000, except for the specimen in Fig. 1E which was obtained with a Philips CM12S microscope equipped with a secondary electron detector.

Transmission electron microscopy (TEM)

Samples of hatching embryos were fixed by adding one volume of 5% glutaraldehyde in artificial sea water (ASW; 454 mM NaCl, 9.7 mM KCl, 9.6 mM $CaCl_2$, 26.7 mM $MgCl_2$, 28.9 mM $MgSO_4$, 5 mM $NaHCO_3$, pH 8). Alternatively, embryos 2 hours old were incubated with exogenous hatching enzyme for varying periods of time and then fixed as described above. Embryos were then quick-frozen, deep-etched, rotary-shadowed as previously described (Mozingo and Chandler, 1991) or post-fixed with osmium tetroxide (1%), en bloc-stained with uranyl acetate (1%), dehydrated in ethanol and embedded in Spurr's resin. Sections cut with a diamond knife were stained with uranyl acetate and lead citrate. Replicas were photographed in stereo using a eucentric goniometer stage on a Philips CM12S microscope; specimens were tilted ±7°.

RESULTS

Scanning electron microscopy of hatching embryos

Hatching begins 17-20 hours after fertilization in *S. purpuratus* and *L. pictus* embryos. Initially, a small proportion of the embryos begin to spin within the confines of the FE and then hatch out. Approximately 2 hours must elapse until the entire culture has completed the hatching process. Hatching in *S. purpuratus* embryos was examined by preparing samples for scanning electron microscopy (SEM) from cultures mid-way through the hatching process. At this time some embryos are still completely encased in the FE (not shown), whereas the hatching process has already begun in other embryos (Fig. 1A). Initially one or several tears in the FE appear (Fig. 1A) which are surrounded by small holes ranging from about 0.17-2.9 μm in size (Fig. 1B, arrows). Tears in the FE are progressively expanded by the beating cilia (Fig. 1C) until the embryo is almost completely free of the FE (Fig. 1D). The FEs left behind from embryos which have completed the hatching process illustrate the patchwork nature of the degradation process (Fig. 1E). In some areas the FE is still largely intact (asterisks), while in other areas the FE is riddled with small gaps or entirely degraded (Fig. 1E).

Hatching in vivo

Proteolytic degradation of the FE by hatching enzyme was examined by preparing hatching embryos for quick-freeze/deep-etch/rotary-shadowing (QF/DE/RS) or thin-sectioning. Prior to hatching, *S. purpuratus* FEs consist of a contiguous paracrystalline layer covering both the microvillar casts and the regions between (not shown, see Chandler and Heuser, 1980). During hatching, the first detectable change in the FE is the appearance of a series of tiny holes where paracrystalline material has been removed (Fig. 2A, arrowheads), although in most areas paracrystalline material is undisturbed (Fig. 2A). Removal of paracrystalline material becomes more extensive as hatching proceeds, exposing the underlying central layer (Fig. 2B, arrowheads). The central layer appears to be composed of a loose network of thin fibers, quite unlike the thick central layer present in completed envelopes (Chandler and Kazilek, 1986; Mozingo and Chandler, 1992), suggesting that macromolecules have also been removed from this layer during hatching.

In *L. pictus* embryos, the paracrystalline layer was also attacked by hatching enzyme, although two different patterns of degradation were observed. One pattern consists of roughly rectangular patches of intact paracrystalline material that splay apart along their borders into fibers as though depolymerizing (Fig. 3A, arrowhead). The paracrystalline material observed beneath these degraded areas illustrates

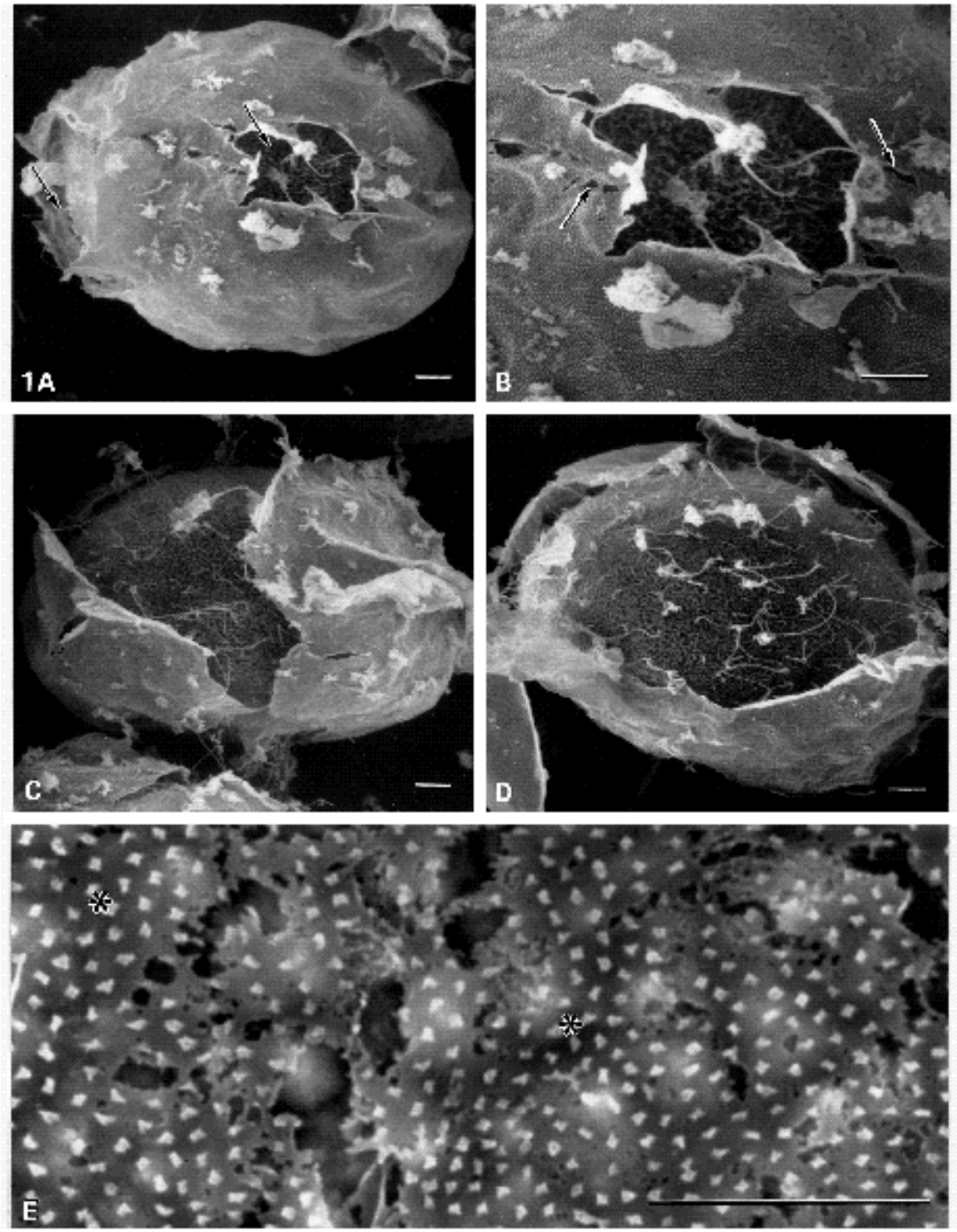

Fig. 1. Scanning electron micrographs of *S. purpuratus* embryos hatching out of their FEs 19.5 hours after fertilization. (A) One or several small tears in the FE (arrows) indicate an embryo which is just beginning the hatching process. (B) Higher magnification shows a central tear rimmed by a series of smaller holes (arrows). (C) In this embryo, tears in the FE have been progressively enlarged by the beating cilia. (D) An embryo which is almost free from the confines of the FE. (E) A FE left behind after embryo hatching, indicating the patchwork nature of the degradation process. Asterisks indicate regions where the FE is still largely intact. The round reflective areas are due to irregularities in the surface of the grid. Bars, 5.0 μm.

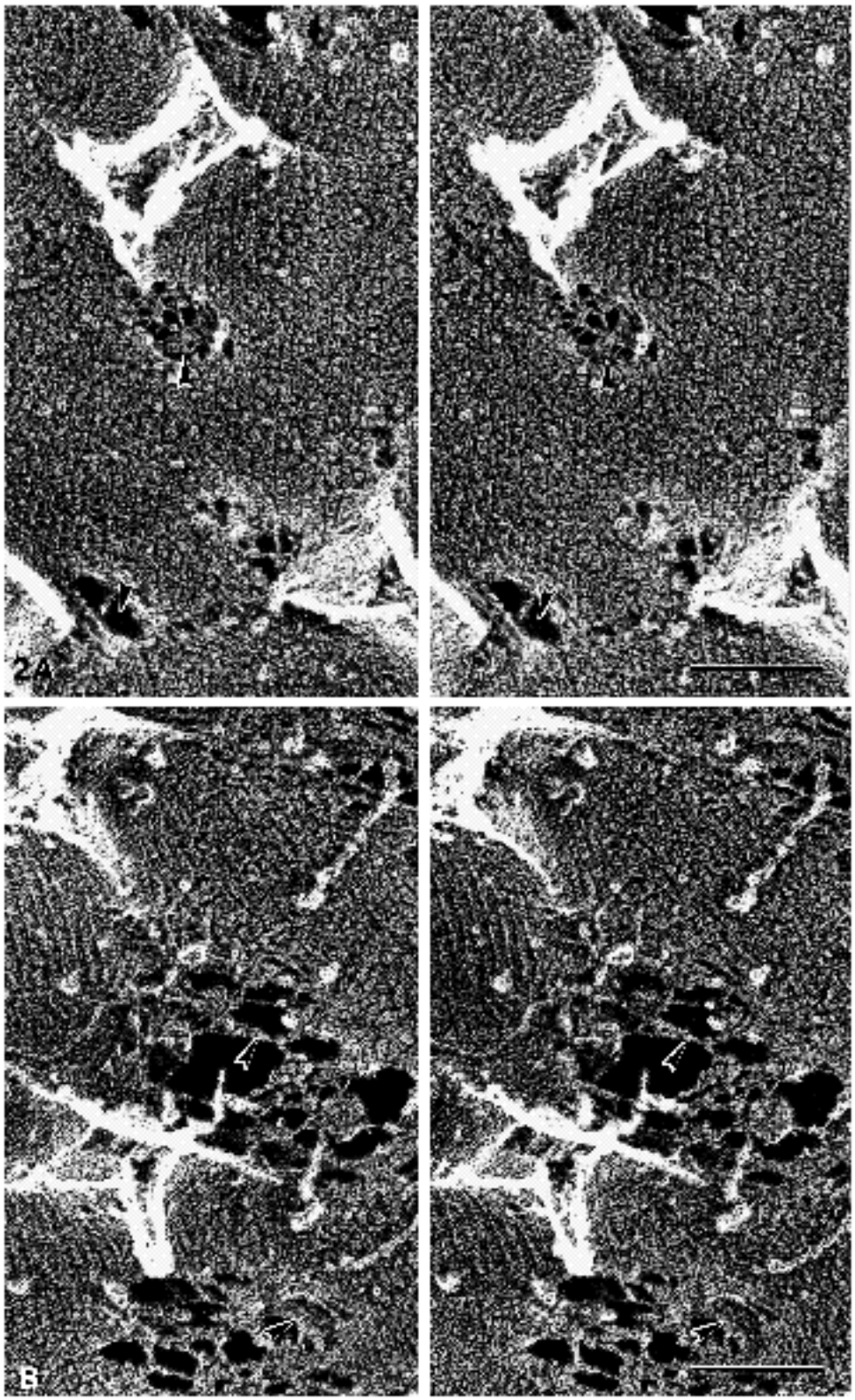

Fig. 2. Quick-freeze/deep-etch/rotary-shadow platinum replicas of *S. purpuratus* FEs during hatching. The angular projections are microvillar casts. (A) The paracrystalline layer is largely intact during the early stages of hatching; however, patches of paracrystalline material have been removed in some regions (arrowheads). (B) In more severely degraded envelopes, paracrystalline material has been removed from larger areas and fibers from the central layer can be seen underneath (arrowheads). Stereo pairs. Bars, 0.2 μm.

the multilamellar nature of the paracrystalline coat in this species. In other areas, the paracrystalline layers appear to be peeling away in patches (Fig. 3B). Adhering to these patches is a thin layer with a fibrous appearance (Fig. 3B, arrowhead) which may facilitate bonding of the paracrystalline multi-layers.

Thin sections reveal hatching-associated changes in the FE which correspond to freeze-fracture observations. During hatching in *S. purpuratus*, FEs exhibit sporadic patches where paracrystalline material has been removed (Fig. 4A, arrowhead), although this layer is often undisturbed in neighboring regions (Fig. 4A). As degradation

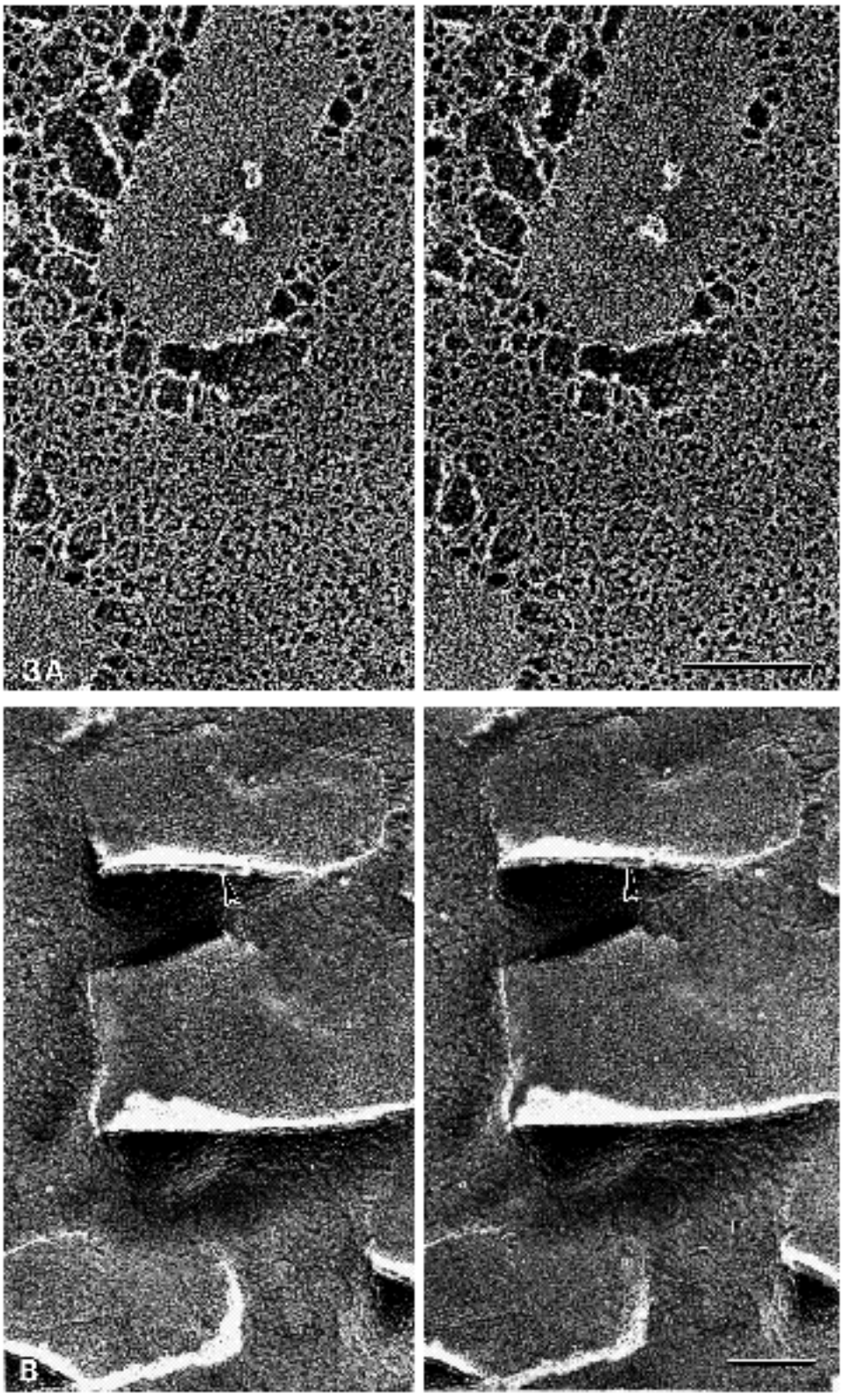

Fig. 3. Platinum replicas of *L. pictus* FEs illustrating the two patterns of degradation observed during hatching. Microvillar casts are not present in this species. (A) Intact paracrystalline material occurs in patches which are splayed apart into fibers along their borders (arrowhead). (B) In some regions of the envelope, paracrystalline material is stripped away in sections. Material with a fibrous appearance can be seen adhering to the underside of the paracrystalline layer (arrowhead). Stereo pairs. Bars, 0.2 μm.

progresses, disruption of the paracrystalline layers becomes more extensive and the previously dense central layer is transformed into a loose array of fibers (Fig. 4B).

The intensely staining paracrystalline layers in *L. pictus* are initially degraded in small patches (Fig. 4C, arrowhead). In severely degraded envelopes, paracrystalline material is absent except for a few scattered patches (Fig. 4E, arrowhead) and the central layer consists of a loose aggregation of filaments. The FEs of hatching embryos sometimes exhibit a multi-lamellar appearance. In some areas, the

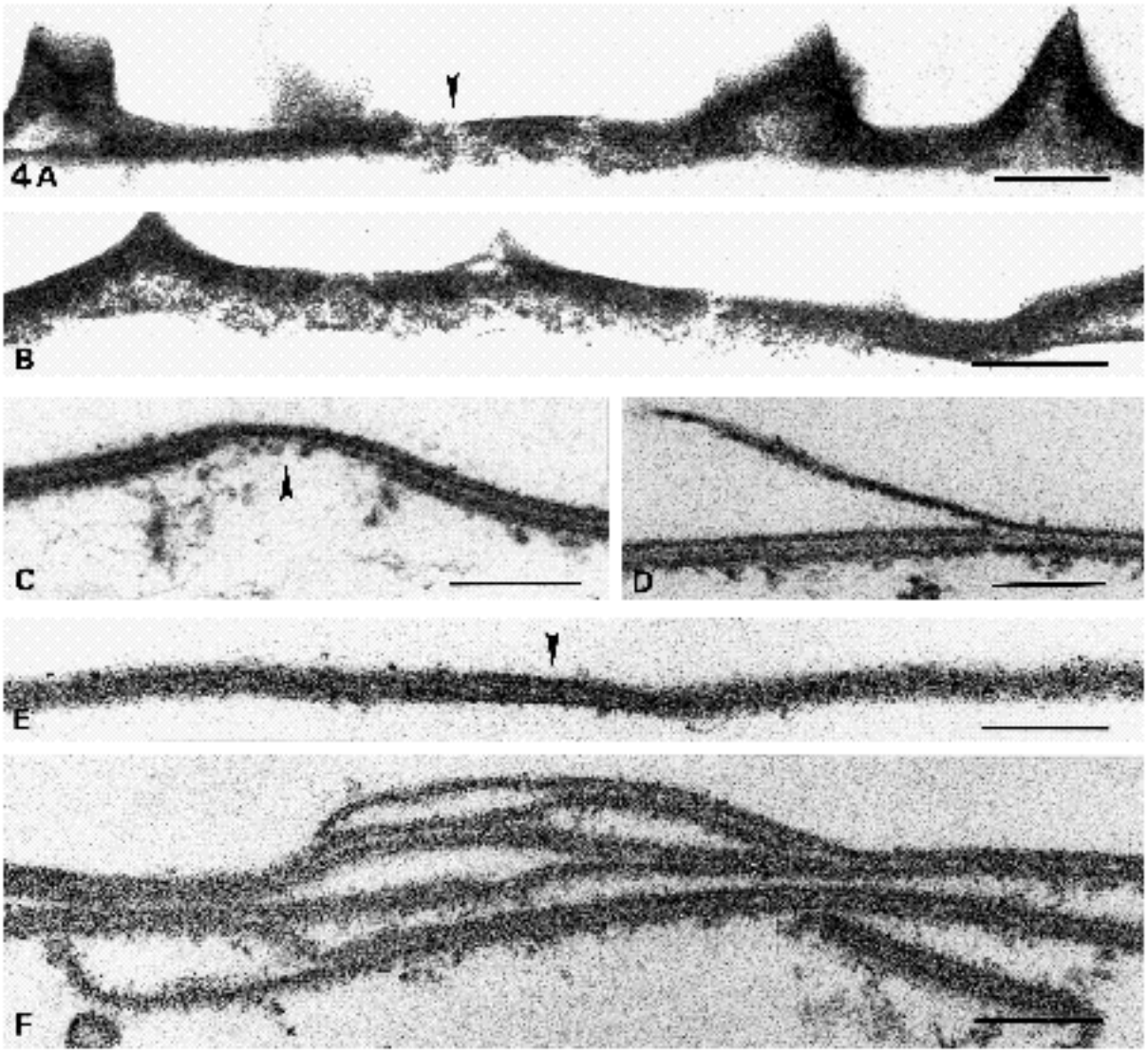

Fig. 4. Thin sections of *S. purpuratus* and *L. pictus* FEs during hatching. (A) Initially small patches of the paracrystalline layer are removed by hatching enzyme (arrowhead). (B) In severely degraded envelopes the paracrystalline layers are disrupted and the central layer appears as an open-weaved meshwork of fibers. (C) Likewise in *L. pictus* FEs, small patches of paracrystalline material (arrowhead) are removed first. (D) In some areas, strips of the paracrystalline coat can be seen peeling away from the FE. (E) In severely degraded envelopes paracrystalline material is absent in all but a few places (arrowhead) and the central layer consists of a loose aggregation of filaments. (F) In some areas the *L. pictus* FE forms multiple layers. Bars, 0.2 μm.

paracrystalline coat appears to be peeling away (Fig. 4D) in a manner similar to that seen by QF/DE/RS methods (Fig. 3B). In other areas, complex patterns of multiple paracrystalline layers are seen (Fig. 4F). Although their relationship to hatching is not clear, it is possible that these multiple layers are formed by partially degraded paracrystalline proteins.

Hatching in vitro

We used an in vitro system to confirm that hatching enzyme was responsible for the observed changes in the FE during natural hatching, and to obtain a temporal sequence of the changes in FE ultrastructure elicited by hatching enzyme. Hatching enzyme collected from *S. purpuratus* embryos (see Materials and Methods) was applied to embryos 2 hours after fertilization, well in advance of synthesis or secretion of endogenous hatching enzyme (Roe and Lennarz, 1990). Samples withdrawn at a series of incubation times were prepared for QF/DE/RS or thin-sectioning. A 30 minute incubation with hatching enzyme leads to disruption or complete removal of the paracrystalline layer from some areas, similar to the results obtained during natural hatching (Fig. 5A). In addition, the thin fibrous nature of the underlying central layer suggests that macromolecules are removed from here as well (Fig. 5A, arrowhead). Although undisrupted paracrystalline material is still present on some envelopes after 60 minutes, it is completely removed in other areas, leaving behind a thin matrix of loosely woven fibers (Fig. 5B). This structure resembles a vitelline layer which has elevated off the egg surface but

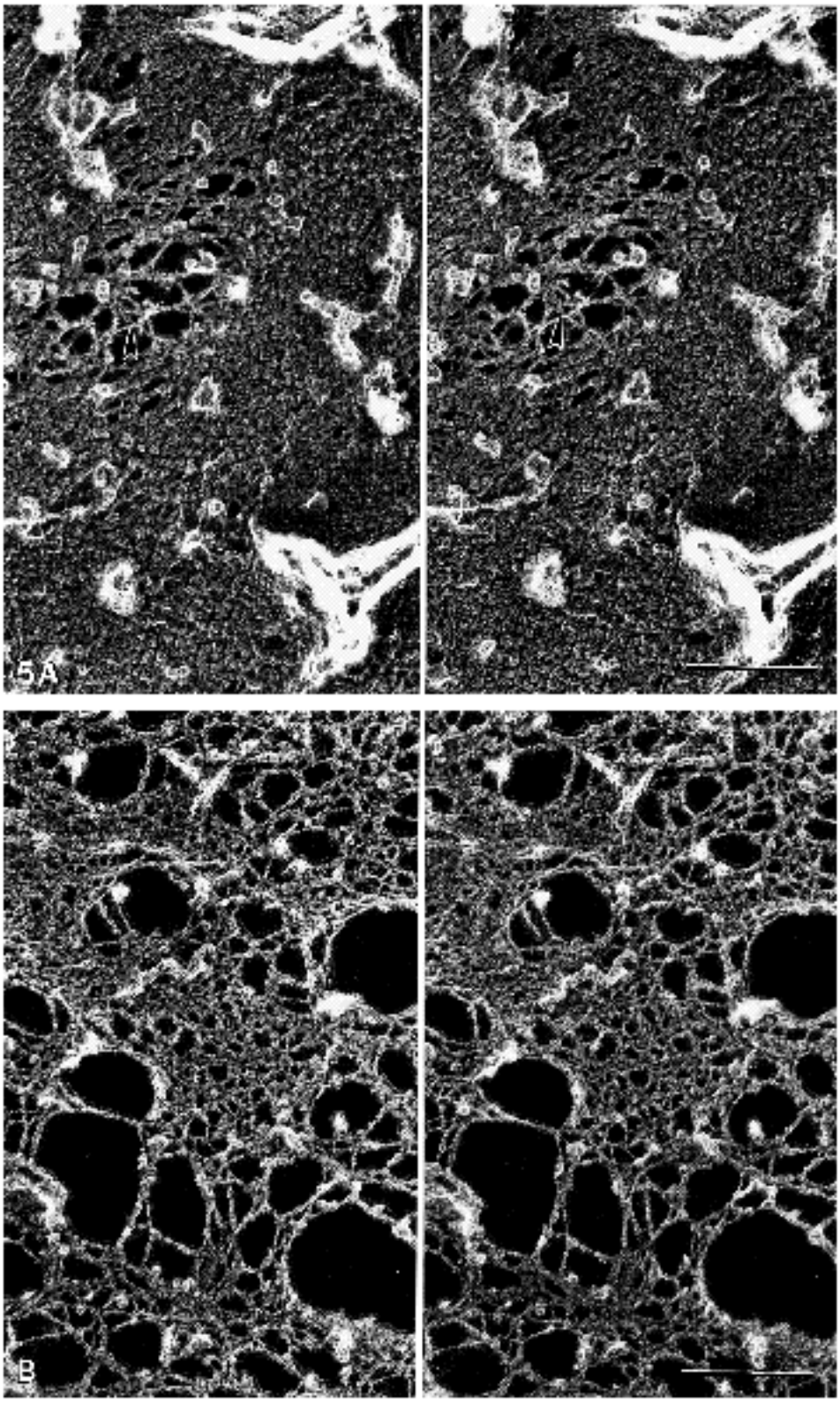

Fig. 5. Platinum replicas of *S. purpuratus* FEs during *in vitro* hatching. (A) After a 30 minute incubation with hatching enzyme, paracrystalline material has been removed from some regions revealing the fibrous core below (arrowhead). (B) After 60 minutes, paracrystalline material has been completely removed from some FEs, leaving behind a thin matrix of loosely woven fibers. Additionally, microvillar casts have degenerated. Stereo pairs. Bars, 0.2 μm.

has not been modified by cortical granule secretions (Chandler and Heuser, 1980; Mozingo and Chandler, 1992). In addition, removal of paracrystalline material may cause the microvillar casts to degenerate since these structures are no longer visible. In contrast, when embryos were incubated with boiled hatching enzyme, no changes in FE ultrastructure were observed, even after 2 hours (not shown).

Thin sections of FEs hatched in vitro also indicated that degradation begins with the removal of small patches of paracrystalline material (Fig. 6A, arrowhead). Subsequent

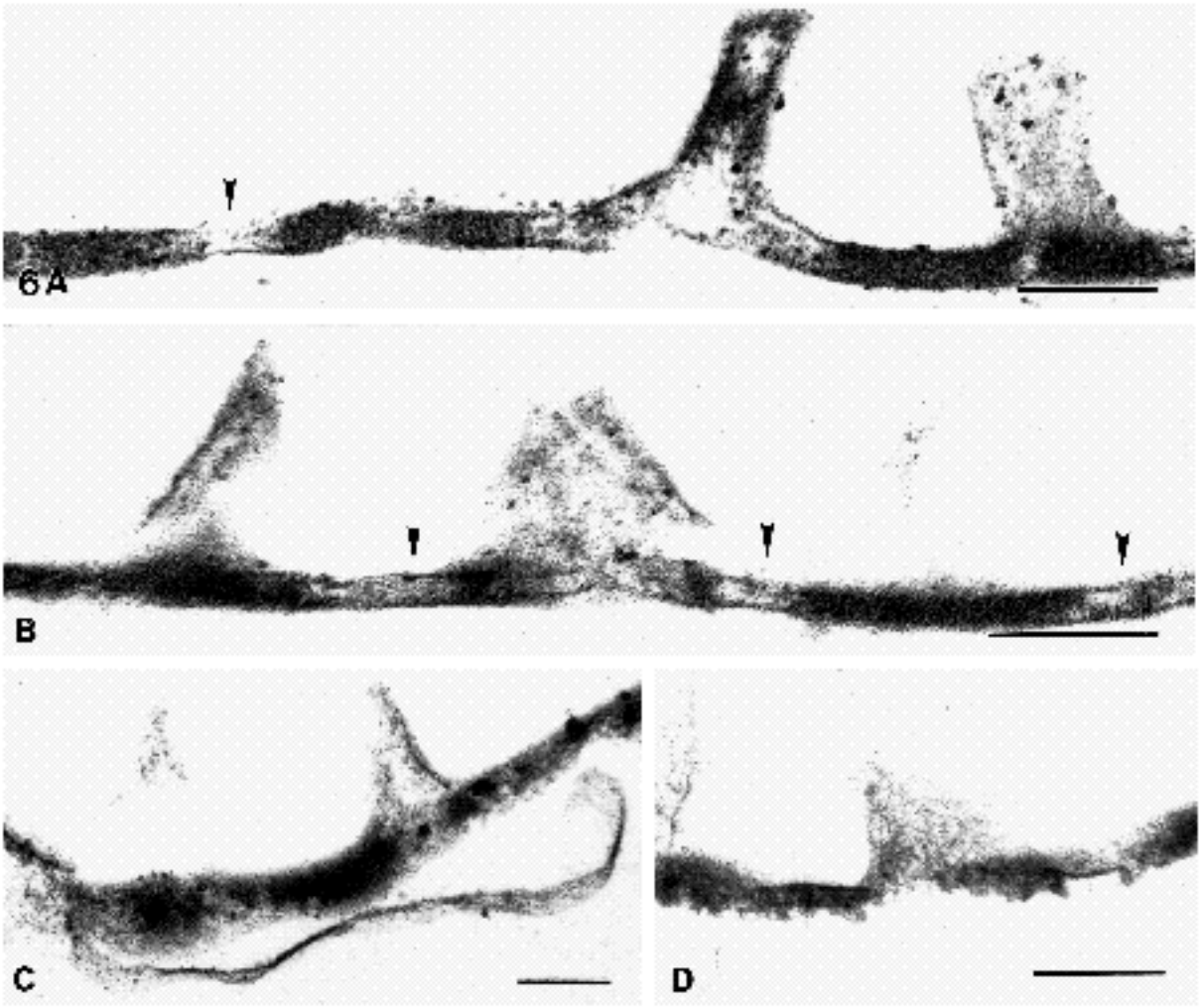

Fig. 6. Transmission electron micrographs of *S. purpuratus* FEs during *in vitro* hatching. (A) After a 30 minute incubation with hatching enzyme, partial removal of the paracrystalline coat is evident (arrowhead). (B) After 40 minutes, the areas undergoing degradation encompass a larger portion of the FE (arrowheads). (C) A 60 minute incubation with hatching enzyme gives rise to regions where large sections of paracrystalline material peel away. (D) FEs incubated with hatching enzyme for 60 minutes are nearly devoid of paracrystalline protein including the degenerated microvillar casts. Bars, 0.2 μm.

enzyme activity results in the removal of material from the central layer; in fact in some areas extensive removal of macromolecules from this layer renders it electron-lucent (Fig. 6B, arrowheads). In some regions we observed large sections of paracrystalline material peeling away from the inner side of the degraded FE (Fig. 6C). This suggests that although the enzyme is applied to the outer surface of the FE, once it has penetrated the FE it can degrade the FE from within the perivitelline space. Severely degraded envelopes are almost completely devoid of paracrystalline material, including the casts which display a fibrous appearance (Fig. 6D).

DISCUSSION

The sea urchin fertilization envelope consists of a central layer of densely-packaged filaments encased by a morphologically distinct paracrystalline coat (Chandler and Heuser, 1980). In this study, we examined ultrastructural changes in the FE initiated by hatching enzyme. In scanning electron micrographs of hatching *S. purpuratus* embryos, we found that holes of various sizes were produced in the FE. TEM methods revealed that these holes corresponded to patches of envelope where paracrystalline material had been removed, whereas adjacent areas of this layer were left intact. In regions where the paracrystalline coat is absent, the central layer was composed of thin, sparsely distributed fibers suggesting that macromolecules had been removed from this layer as well. Similar results were obtained when exogenous hatching enzyme was applied to embryos well in advance of the hatching stage.

The ultrastructural changes we observed in both layers of the FE led us to conclude that hatching enzyme degrades the FE by disrupting the paracrystalline layers and removing macromolecules from the central layer. Indeed, in severely degraded envelopes, paracrystalline material is entirely absent and all that remains of the central layer is

a thin network of loosely woven fibers (Fig. 5B). Hatching in *L. pictus* proceeds by a similar mechanism although some differences are worth noting. In this species, we observed expanses of envelope where paracrystalline material was peeling away, suggesting that this matrix is disassembled, in part, by removal of large sections of envelope. The proposed pattern of FE degradation by hatching enzyme is supported by studies which describe biochemical changes in *S. purpuratus* FEs during hatching. Using immunoblotting to characterize hatching-associated changes in the FE, Uher and Carroll (1987) found that hatching enzyme cleaves the paracrystalline protein fraction from the FE.

With the exception of the Ca^{2+}-dependent ovoperoxidase-binding protein, proteoliaisin, the in vivo protein substrates of ovoperoxidase-catalyzed cross-linking have not been identified (Kay and Shapiro, 1987). However, ultrastructural evidence suggests that the protein(s) which gives rise to the paracrystalline layers is incorporated into the nascent FE by ovoperoxidase (Mozingo and Chandler, 1991). The present study indicates that hatching enzyme degrades the paracrystalline layers and, in an SDS-PAGE analysis of the FE proteins proteolyzed by hatching enzyme, Roe and Lennarz (1990) showed that many of the FE proteins targeted for degradation by hatching enzyme are those incorporated into the FE by ovoperoxidase. Thus, it appears that at least a subset of the proteins removed from the FE during hatching are the same as those cross-linked into the vitelline scaffold by ovoperoxidase during FE assembly.

Hatching enzyme is a metalloendoprotease homologous to vertebrate extracellular matrix-degrading enzymes including the collagenases and stromelysins (Lepage and Gache, 1990). The purified enzyme alone can dissolve FEs in vitro (Lepage and Gache, 1989), although hatching in vivo may involve the activity of several factors. Firstly, an additional metalloendoprotease has recently been identified which is probably secreted in concert with hatching enzyme, suggesting it may also play a role during hatching (Reynolds et al., 1992). Indeed, degradation of the chorion surrounding the medaka (*Oryzias latipes*) embryo is effected by the action of two metalloproteases acting cooperatively (Yasumasu et al., 1988). A chymotrypsin-like enzyme has also been implicated during hatching in sea urchin embryos. Purified hatching enzyme is not affected by chymotrypsin inhibitors (Barrett and Edwards, 1976; Takeuchi et al., 1979), but specific inhibitors of chymotrypsin have been found to inhibit the natural hatching process as well as *in vitro* degradation of the FE by crude hatched blastula culture media (Hoshi et al., 1979; Post et al., 1988). Although the role of additional factors during hatching has not been determined, it is interesting to speculate that the morphologically distinct layers of the FE may be degraded by separate enzymes.

The hatching enzyme gene is one of the earliest transcribed from the zygotic genome. Expression of this gene is tightly controlled, both temporally and spatially, by the developing embryo. Hatching enzyme is not present in eggs and adult tissues and makes but a brief appearance during early development (Lepage and Gache, 1990; Reynolds et al., 1992). Levels of hatching enzyme mRNA begin to appear as early as the 8-cell stage, reach peak abundance during the 128-cell stage and disappear by the mesenchyme blastula stage (Lepage and Gache, 1990; Reynolds et al., 1992). Activation of the hatching enzyme gene appears to be cell autonomous since intercellular contacts are not required; however, down-regulation may require cell-cell contacts (Reynolds et al. 1992). Immunolabeling and in situ hybridization using RNA probes both reveal a remarkable pattern of spatial expression. Hatching enzyme is only produced by cells in the animal-most two-thirds of the embryo (Lepage et al., 1992; Reynolds et al., 1992). The significance of this finding to the hatching process is not yet known, however, Uher and Carroll (1987) noted that embryos hatch out of the FE with an intriguing polarity. The FE appears to weaken most noticeably on one side, but it is not known whether this region corresponds to the animal pole of the embryo.

Degradation of the FE by hatching enzyme is in some ways reminiscent of assembly of this matrix at fertilization. Firstly, it appears that a subset of the cortical granule proteins cross-linked into the vitelline scaffold by ovoperoxidase at fertilization are targeted for removal by hatching enzyme (Roe and Lennarz, 1990; this study). In addition, the striking similarity between FEs that have been severely degraded by hatching enzyme (Fig. 5B) and elevated vitelline layers that have not been modified by cortical granule secretions (Chandler and Heuser, 1980; Mozingo and Chandler, 1992) suggests that these two structures may be related. Moreover, hatching enzyme apparently has no effect on the vitelline layer (Kopac, 1941), although this observation awaits confirmation at the ultrastructural level.

The programmed assembly of the FE (which renders the egg unfertilizable by supernumerary sperm) and the disassembly of this matrix (which allows the motile blastula to swim free), underscore the vital role extracellular matrices play during development. In the sea urchin, two additional extracellular matrices are assembled and remodeled during development. The hyaline layer is assembled at fertilization and continues to surround the embryo throughout embryogenesis; however, it is extensively remodeled at the blastula stage and during gastrulation and pluteus formation (Bisgrove et al., 1991). The hyalin layer holds the dividing blastomeres together and plays an essential role during blastocoel formation and gastrulation (reviewed by McClay et al., 1990). Another distinct extracellular matrix lines the blastocoel and closely resembles vertebrate basal lamina (McClay et al., 1990). Remodeling of this matrix by increased deposition of collagen is necessary for gastrulation to occur (Wessel and McClay, 1987). In vertebrates, remodeling of the extracellular matrix has been observed in many developmental processes. In particular, metalloendoproteases have been shown to participate in tadpole tail reabsorption (Gross and Lapiere, 1962), branching morphogenesis (Nakanishi et al., 1986) and implantation of the mammalian embryo in the uterine epithelium (Librach et al., 1991). Thus, FE assembly and subsequent degradation by a metalloprotease is typical of extracellular matrices' life histories during which specialized matrices are assembled, function within restricted time and space, and are then degraded to make way for the next matrix.

We thank Dr Richard Trelease for helpful advice and for pro-

viding the Amicon ultrafiltration system. This study was supported by NSF grant IBN-9117509.

REFERENCES

Barrett, D. and Edwards, B.F. (1976). Hatching enzyme of the sea urchin *Strongylocentrotus purpuratus.* In *Methods in Enzymology*, vol. 45 (ed. L. Lorand), pp. 354-373. New York: Academic Press.

Bisgrove, B.W., Andrews, M.E. and Raff, R.A. (1991). Fibropellins, products of an EGF repeat-containing gene, form a unique extracellular matrix structure that surrounds the sea urchin embryo. *Dev. Biol.* **146**, 89-99.

Carroll, E.J. and Cohen, J.S. (1990). A comparison of fertilization envelope development in three species of *Strongylocentrotus* (*S. franciscanus, S. droebachiensis* and *S. purpuratus*). *Mol. Reprod. Dev.* **25**, 77-86

Carroll, E.J. and Epel, D. (1975). Isolation and biological activity of the proteases released by sea urchin eggs following fertilization. *Dev. Biol*. **44**, 22-32.

Chandler, D.E. and Heuser, J. (1980). The vitelline layer of the sea urchin egg and its modification during fertilization. *J. Cell Biol.* **84**, 618-632.

Chandler, D.E. and Kazilek C.J. (1986). Extracellular coats on the surface of *Strongylocentrotus purpuratus* eggs: stereo electron microscopy of quick-frozen deep-etched specimens. *Cell Tiss. Res.* **246**, 153-161.

Foerder, C.A. and Shapiro, B.M. (1977). Release of ovoperoxidase from sea urchin eggs hardens the fertilization membrane with tyrosine crosslinks. *Proc. Nat. Acad. Sci. USA* **74**, 4214-4218.

Glabe, C.G. and Vacquier, V.D. (1978). Egg surface glycoprotein receptor for sea urchin sperm binding. *Proc. Nat. Acad. Sci. USA* **75**, 881-885.

Gross, J. and Lapiere, C.M. (1962). Collagenolytic activity in amphibian tissues: a tissue culture assay. *Proc. Nat. Acad. Sci. USA* **48**, 1014-1022.

Hall, H.G. (1978). Hardening of the sea urchin fertilization envelope by peroxidase-catalyzed phenolic coupling of tyrosines. *Cell* **15**, 343-355.

Hoshi, M., Moriya, T., Aoyagi, T. and Umezawa, H. (1979). Biochemical studies of the hatching process in sea urchin embryos. *J. Exp. Zool.* **209**, 129-134.

Ishida, J. (1936). An enzyme dissolving the fertilization membrane of sea urchin eggs. *Annot. zool. jap.* **15**, 453-459.

Kay, E.S. and Shapiro, B.M. (1985). The formation of the fertilization membrane of the sea urchin egg. In *Biology of Fertilization*, vol. 3 (ed. C.B. Metz and A. Monroy), pp. 45-80. Orlando, FL: Academic Press.

Kay, E.S. and Shapiro, B.M. (1987). Ovoperoxidase assembly into the fertilization envelope and dityrosine crosslinking. *Dev. Biol.* **121**, 325-334.

Kidd, P. (1978). The jelly and vitelline coats of the sea urchin egg: new ultrastructural features. *J. Ultrastruct. Res.* **64**, 204-215.

Kinsey, W.H. and Lennarz, W.J. (1981). Isolation of a glycopeptide fraction from the surface of the sea urchin egg that inhibits sperm-egg binding and fertilization. *J. Cell Biol.* **91**, 325-331.

Kopac, M.J. (1941) Disintegration of the fertilization membrane of *Arbacia* by the action of an enzyme. *J. Cell Comp. Physiol.* **18**, 215-220.

Lepage, T. and Gache, C. (1989). Purification and characterization of the sea urchin embryo hatching enzyme. *J. Biol. Chem.* **264**, 4787-4793.

Lepage, T. and Gache, C. (1990). Early expression of a collagenase-like hatching enzyme gene in the sea urchin embryo. *EMBO J.* **9**, 3003-3012.

Lepage, T., Sardet, C. and Gache, C. (1992). Spatial expression of the hatching enzyme gene in the sea urchin embryo. *Dev. Biol.* **150**, 23-32.

Librach, C.L., Werb, Z., Fitzgerald, M.L., Chiu, K., Corwin, N.M., Esteves, R.A., Grobelny, D., Galardy, R., Damsky, C.H. and Fisher, S.J. (1991). 92-kD Type IV collagenase mediates invasion of human cytotrophoblasts. *J. Cell Biol.* **113**, 437-449.

Longo, F.J. and Schuel, H. (1973). An ultrastructural examination of polyspermy induced by soybean trypsin inhibitor in the sea urchin *Arbacia punctulata. Dev. Biol.* **34**, 187-199.

McClay, D.R., Alliegro, M.C. and Black, S.D. (1990). The ontogenetic appearance of extracellular matrix during sea urchin development. In *Organization and Assembly of Plant and Animal Extracellular Matrix*, (ed. W.S. Adair and R.P. Mecham), pp. 1-13. San Diego, CA: Academic Press.

Morrill, J.B. (1986). Scanning electron microscopy of embryos. In *Methods in Cell Biology*, vol. 27 (ed. T.E. Schroeder), pp. 263-293. Orlando, FL: Academic Press.

Mozingo, N.M. and Chandler, D.E. (1991). Evidence for the existence of two assembly domains within the sea urchin fertilization envelope. *Dev. Biol.* **146**, 148-157.

Mozingo, N.M. and Chandler, D.E. (1992). Ultrastructural changes during fertilization envelope assembly in *Lytechinus pictus* eggs revealed by quick-freeze, deep-etch electron microscopy. *Cell Tiss. Res.* (in press).

Nakanishi, Y., Sugiura, F., Kishi, J.-I. and Hayakawa, T. (1986). Collagenase inhibitor stimulates cleft formation during early morphogenesis of mouse salivary gland. *Dev. Biol.* **113**, 201-206.

Post, L.L., Schuel, R. and Schuel, H. (1988). Evidence that hatching enzyme of the sea urchin *Strongylocentrotus purpuratus* is a chymotrypsin-like protease. *Biochem. Cell Biol.* **66**, 1200-1209.

Reynolds, S.D., Angerer, L.M., Palis, J., Nasir, A. and Angerer, R.C. (1992). Early mRNAs, spatially restricted along the animal-vegetal axis of sea urchin embryos, include one encoding a protein related to tolliod and BMP-1. *Development* **114**, 769-786.

Roe, J.L. and Lennarz, W.J. (1990). Biosynthesis and secretion of the hatching enzyme during sea urchin embryogenesis. *J. Biol. Chem.* **265**, 8704-8711.

Rossignol, D.P., Earles, B.J., Decker, G.L. and Lennarz, W.J. (1984). Characterization of the sperm receptor on the surface of eggs of *Strongylocentrotus purpuratus. Dev. Biol.* **104**, 308-321.

Schuel, H., Schuel. R., Dandekar, P., Boldt, J. and Summers, R. (1982). Sodium requirements in hardening of the fertilization envelope and embryonic development in sea urchins. *Biol. Bull. Mar. Biol. Lab., Woods Hole* **162**, 202-213.

Takeuchi, K., Yokosawa, H. and Hoshi, M. (1979). Purification and characterization of hatching enzyme of *Strongylocentrotus intermedius*. *Eur. J. Biochem.* **100**, 257-265.

Uher, V.I. and Carroll, E.J. (1987). Characterization of hatching-associated changes in the sea urchin fertilization envelope. *Gamete Res.* **16**, 267-279.

Vacquier, V.D. Epel, D. and Douglas, L.A. (1972). Sea urchin eggs release protease activity at fertilization. *Nature* **237**, 34-36.

Veron, M., Foerder, C., Eddy, E.M. and Shapiro, B.M. (1977). Sequential biochemical and morphological events during assembly of the fertilization membrane of the sea urchin. *Cell* **10**, 321-328.

Wessel, G.M. and McClay, D.R. (1987). Gastrulation in the sea urchin embryo requires the deposition of crosslinked collagen within the extracellular matrix. *Dev. Biol.* **121**, 149-165.

Yasumasu, S., Iuchi, I. and Yamagami, K. (1988) Medaka hatching enzyme consists of two kinds of proteases which act cooperatively. *Zool. Sci.* **5**, 191-195.

(Received 15 September 1992 - Accepted 10 November 1992)